Subcritical Swirling Flows in Convergent, Annular Nozzles

K. Knowles*
Royal Military College of Science, Shrivenham, United Kingdom
and
P. W. Carpenter†
University of Exeter, Exeter, United Kingdom

A quasicylindrical theory is developed for subcritical, inviscid, swirling flows in annular nozzles and extended to include nonuniiorm stagnation conditions. A small perturbation theory is also developed and shown to give remarkably good agreement, even for high swirl levels. The effects on mass flow rate, impulse function, and thrust of different swirl velocity profiles are investigated for a typical turbofan geometry, with nonswirling core nozzle flow, at differing nozzle pressure ratios. Specific thrust is found to decrease with swirl. The rate of decay depends on the swirl velocity profile, and the relative effects of different swirl profiles depend on the basis of comparison.

Nomenclature

a	= speed of sound
A	= area of nozzle
$A...E$	= coefficients used in thrust equation, Eq. (11)
A_e	= πR_e^2
C_m	= mass flux coefficient
C_n	= impulse function
C_{pe}	= $(p_b - p_a)/\frac{1}{2}\rho V_F^2$
C_{st}	= coefficient of specific thrust
C_t	= coefficient of thrust
F_1, F_2	= coefficients used in thrust equation, Eq. (11)
h	= enthalpy
I_2	= integral given in Eq. (16)
p	= pressure
q	= total velocity $(\sqrt{v^2 + w^2})$
Q	= q/a_*
r	= radial coordinate
R_e	= outer radius of fan nozzle, Fig. 1
R_{ex}	= outer radius of core nozzle, Fig. 1
R_{e2}	= outer radius of fan stream at plane 2, Fig. 1
R_i	= inner radius of fan nozzle, Fig. 1
s	= entropy
S, S_A, S_B, S_D, S_1, S_2, S_3	= swirl parameters, Eqs. (2, 13, 14, 17, and 25)
S'	= $\int_{R_i}^{R_e} wvr^2 dr / (R_e \int_{R_i}^{R_e} w^2 r\, dr)$
t	= thrust
T	= temperature
v	= swirl velocity
v_F	= flight velocity
V	= v/a_*
V_F	= v_F/a_{*c}
w	= axial velocity
W	= w/a_*
γ	= ratio of specific heats
δp_0	= local departure of stagnation pressure from reference (lip) value, Eq. (19)
Δp_0	= total variation of stagnation pressure for linear profile, Eq. (26)
ΔP	= $\Delta p_0/p_{0e}$
θ	= swirl angle
Λ	= nozzle lip pressure ratio parameter, Eq. (14)
ξ	= nondimensionalized radius r/R_e
ρ	= density

Subscripts

a	= ambient conditions
b	= conditions in external stream at fan nozzle lip
c	= conditions in core stream
cowl	= conditions on afterbody cowl, Fig. 1
e	= conditions at fan nozzle lip
e_2	= conditions on outside of fan stream at station 2, Fig. 1
ex	= conditions at core nozzle lip
f	= conditions in fan stream
i	= conditions on inside of fan nozzle
max	= maximum value
0	= stagnation conditions
1	= fan nozzle exit plane, Fig. 1
2	= conditions in fan stream at core nozzle exit plane, Fig. 1
*	= critical conditions

Introduction

CONVERGENT, annular propulsion nozzles are widely used for the fan stream of high-bypass-ratio turbofan engines. There is an interest in determining the effects of swirl on such nozzles due to the presence of residual swirl from the fan. Furthermore, earlier studies,[1-5] which were aimed at noise reduction,[6,7] showed the possibility of using swirl to control mass flow with minimal effect on specific thrust. This may be useful in influencing off-design performance[8].

Effects of swirl can be investigated most readily by extending the classical quasicylindrical theory for compressible, inviscid nozzle flows. Such an approach models pressure gradients due to swirl but neglects those due to streamline curvature and so is strictly applicable only to slender nozzles or dominant swirl. It is, however, satisfactory for the purposes of a feasibility study, particularly since wall curvature opposes swirl (so that the present method tends to overestimate swirl effects). To investigate the effects of fan residual swirl, the theory needs to be extended further to include nonuniform stagnation pressure effects. This has been done for supercritical flow in convergent-divergent nozzles,[2] and that method is extended to subcritical convergent annular nozzle flows here.

Received April 24, 1987.

*Lecturer, Aeromechanical Systems Group, School of Mechanical, Materials and Civil Engineering. Member AIAA.
†Reader, School of Engineering. Member AIAA.

Previous studies of swirling propulsive flows have concentrated on supercritical convergent-divergent nozzles (e.g., Refs. 9-12), using a variety of methods from quasi-one-dimensional,[9] through the method of characteristics (with a series expansion to allow for nozzle curvature[12]), to time marching.[11] An extensive survey is contained in Ref. 1 and updated in Refs. 2-4. Most recently, Kornblum et al.[13] published results for supercritical swirling flows in annular, convergent-divergent nozzles. They used a time-dependent method to define the (curved) sonic line and a method of characteristics scheme for the supersonic flow. Their analysis was limited to the special case of a free vortex. No previous results have been found for the case presented here, with subcritical swirling flow in a convergent, annular nozzle.

Analysis for Uniform Stagnation Conditions

It is assumed that the effects of nozzle wall curvature can be ignored so that the flow at the nozzle exit is equivalent to that in an infinitely long cylindrical duct. It is also assumed, for this part of the analysis, that the swirl velocity is introduced by stationary blades so that (for an inviscid, non-heat-conducting gas) the entropy and stagnation enthalpy are uniformly constant throughout the flow. Using the same assumptions, Carpenter and Johannesen[1] have shown that the Crocco vorticity theorem reduces to

$$\frac{v}{r}\frac{\mathrm{d}(vr)}{\mathrm{d}r} + w\frac{\mathrm{d}w}{\mathrm{d}r} = 0 \tag{1}$$

Integrating Eq. (1) across the exit plane of an annular nozzle and nondimensionalizing velocities by a_* gives

$$W = (Q_e^2 - V_e^2 + 2S)^{1/2} \tag{2}$$

where

$$S = \int_{r_1}^{R_e} \frac{V}{r'}\frac{\mathrm{d}(Vr')}{\mathrm{d}r'}\,\mathrm{d}r'$$

The pressure p and density ρ at the nozzle exit plane are obtained from the isentropic relations, namely,

$$\left(\frac{\rho}{\rho_0}\right)^{\gamma-1} = \left(\frac{p}{p_0}\right)^{(\gamma-1)/\gamma} = 1 - \frac{\gamma-1}{\gamma+1}(W^2 + V^2) \tag{3}$$

These relationships also allow the term Q_e in Eq. (2) to be evaluated, since at the nozzle lip $p = p_a$, the ambient pressure.

Before performance parameters can be developed, the effect of a swirling fan stream on the core nozzle buried within it needs to be considered. In general, swirl produces a static pressure gradient across the stream, thereby reducing the back pressure for the core nozzle. The present approach has been to specify a swirl velocity profile at the fan nozzle exit and then to determine conditions downstream in the plane of the core nozzle exit. Thus, conservation of angular momentum between planes 1 and 2 (see Fig. 1) gives

$$V_2 r_2 = V_1 r_1 \tag{4}$$

Streamline positions at plane 2 can be determined from conservation of mass as

$$r_2 = \left\{R_{e2}^2 - 2\int_{r_1}^{R_e}\left(\frac{\rho_1 W_1 r_1'}{\rho_2 W_2}\right)\mathrm{d}r_1'\right\}^{1/2} \tag{5}$$

Assuming that total velocity remains constant on the jet boundary (this will be discussed when post-exit thrust is considered) and using Eq. (4), Eq. (2) becomes

$$W_2 = \left\{Q_e^2 - V_{e2}^2 + 2\int_{r_1}^{R_e}\frac{V_1 r_1'}{r_2^2}\frac{\mathrm{d}(V_1 r_1')}{\mathrm{d}r_1'}\,\mathrm{d}r_1\right\}^{1/2} \tag{6}$$

Equations (5) and (6) are solved iteratively for r_2.

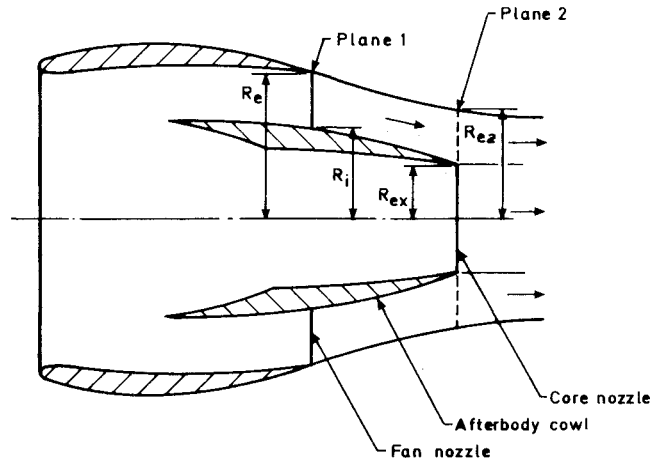

Fig. 1 Turbofan nozzle geometry.

Parameters of most significance in assessing nozzle performance are the mass flux, impulse function and thrust. These can all be cast in nondimensional coefficient form, with the first two being evaluated for each nozzle separately. Thus, the mass flux and impulse function coefficients for the fan nozzle are defined as

$$C_{mf} = 2\int_{R_1}^{R_e}\frac{\rho_f w_f r\,\mathrm{d}r}{\{\rho_{*f} a_{*f} R_e^2\}} \tag{7}$$

and

$$C_{nf} = 2\int_{R_1}^{R_e}\frac{(p_f + \rho_f w_f^2)\,r\,\mathrm{d}r}{\{p_{*f} + \rho_{*f} a_{*f}^2\}R_e^2} \tag{8}$$

respectively. Similar expressions hold for the core nozzle coefficients. The thrust coefficient can be defined as

$$C_t = t/(\rho_{*c} a_{*c}^2\,\pi R_{ex}^2) \tag{9}$$

where core nozzle conditions have been chosen as reference.

For a turbofan engine moving with forward speed V_F, the net standard thrust[14] can be shown to be[15]

$$t = \int_c (p_c + \rho_c w_c^2)\,\mathrm{d}A + \int_f (p_f + \rho_f w_f^2)\,\mathrm{d}A - p_a A_e - v_F\int_c \rho_c w_c\,\mathrm{d}A - v_F\int_f \rho_f w_f\,\mathrm{d}A + \int_{\mathrm{cowl}} p_{\mathrm{cowl}}\,\mathrm{d}A \tag{10}$$

where the subscripts on the integrals indicate integration over the appropriate projected areas.

This expression is obtained by considering the momentum balance for a control volume that extends from infinity upstream laterally sufficiently far that ambient pressure can be considered to act on the sides and downstream to plane 1, then following the afterbody cowl and core nozzle exit. It is assumed, for the time being, that ambient pressure acts everywhere over plane 1 beyond the fan nozzle lip. This assumption, however, will be relaxed when post-exit thrust is considered.

Using Eqs. (7-10), the thrust coefficient can now be written as

$$C_t = AC_{nc} + BC_{nf} + C(p/p_0)_{\mathrm{cowl}} - V_F C_{mc} - V_F DC_{mf} - E \tag{11}$$

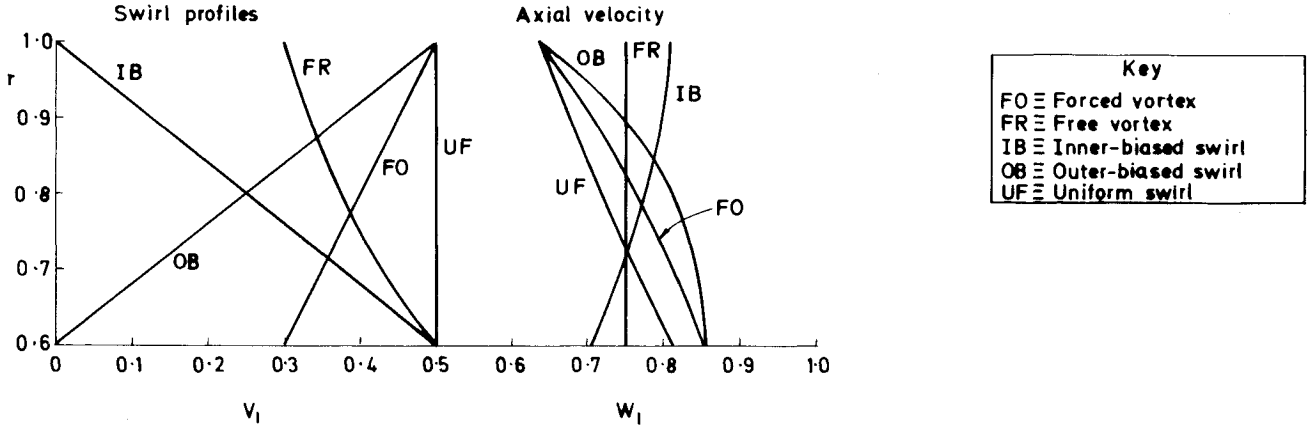

Fig. 2 Velocity profiles for $V_{max} = 0.5$, $p_a/p_{0f} = 1/1.5$.

where

$$A = (\gamma_c + 1)/\gamma_c, \qquad B = (\gamma_f + 1)F_1$$

$$C = (R_i^2 - R_{ex}^2)F_2/(p_a/p_0)_f, \qquad D = \gamma_f(a_{*c}/a_{*f})F_1$$

$$E = F_2 R_e^2$$

$$F_1 = \frac{1}{\gamma_c}\left\{\frac{2}{\gamma_f + 1}\right\}^{\gamma_f/(\gamma_f - 1)}\left\{\frac{\gamma_c + 1}{2}\right\}^{\gamma_c/(\gamma_c - 1)}\left(\frac{p_a}{p_0}\right)_c\left(\frac{p_0}{p_a}\right)_f\left(\frac{R_e}{R_{ex}}\right)^2$$

$$F_2 = \frac{1}{\gamma_c}\left\{\frac{\gamma_c + 1}{2}\right\}^{\gamma_c/(\gamma_c - 1)}\left(\frac{p_a}{p_0}\right)_c\left(\frac{1}{R_{ex}}\right)^2$$

The coefficient of specific thrust is defined as

$$C_{st} = C_t/(C_{mc} + DC_{mf}) \tag{12}$$

The denominator on the right-hand side corresponds to total mass flux nondimensionalized with respect to core conditions.

If the fan nozzle back-pressure ratio is given, then the nondimensional total velocity at fan nozzle lip, Q_e, can be determined from Eq. (3). Hence, if the swirl profile at fan nozzle exit is specified, the axial velocity profile can be determined from Eq. (2). The density and pressure profiles can then be determined from Eq. (3). The fan nozzle mass flux and impulse function coefficients can now be determined numerically from Eqs. (7) and (8).

Conditions in the core nozzle can be found if the nonswirling back-pressure ratio $(p_a/p_0)_c$ is given. The swirl and axial velocity profiles in the fan stream outside the core nozzle exit are determined from Eqs. (4–6); the pressure profile can then be determined from Eq. (3) and this gives the modified back-pressure ratio for the core nozzle. For a nonswirling core stream, as considered here, the axial velocity then follows directly from Eq. (3). Swirling core flows, however, could also be handled, using the same procedure as for the fan stream. In either case, C_{mc} and C_{nc} can now be evaluated numerically.

The thrust coefficient can now be determined from Eq. (11), provided that values can be assigned to V_F, (a_{*c}/a_{*f}), and $(p/p_0)_{cowl}$. For the present calculations the cowl pressure was taken to be the mean of the pressures at either end of the cowl. This is discussed further in Ref. 8. The term (a_{*c}/a_{*f}) can be evaluated from the nonswirling values of the back-pressure ratios and the ratio of fan to core mass flows. The nondimensional forward speed also depends on this ratio and therefore can be evaluated for a specified cruise Mach number. Further discussions of the assumptions and approximations are contained in Ref. 8.

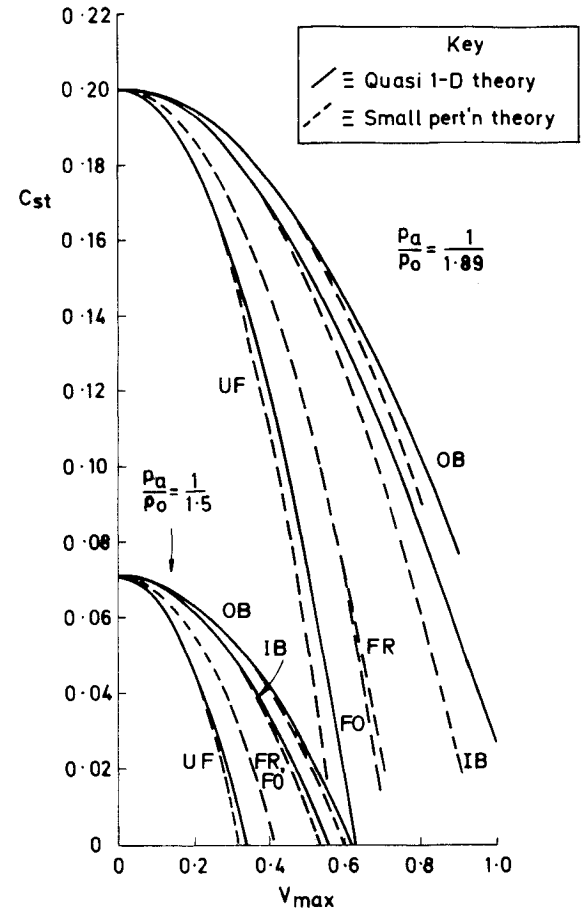

Fig. 3 Variation of specific thrust with swirl velocity for $V_F = 0.4847$ (key as Fig. 2).

Small Perturbation Theory

In the case of weak swirl, analytical expressions can be produced for C_{mf} and C_{nf} by following a procedure similar to that of Carpenter and Johannesen.[1] The right-hand side of Eq. (2) is expanded and terms of $O(V_e^4)$ neglected. Approximate expressions for ρ/ρ_0 and p/p_0 are obtained from Eq. (3) by expanding and neglecting terms of $O(V_e^4)$. These small perturbation approximations for W_f, $(p/p_0)_f$, and $(\rho/\rho_0)_f$ are substituted into definitions (7) and (8) and the integrations carried out, again neglecting terms of $O(V_e^4)$, to obtain the

following approximate expressions for the fan stream:

$$C_{mf} = \{\tfrac{1}{2}(\gamma_f + 1)\Lambda_f\}^{1/(\gamma_f - 1)} Q_e \left\{(1 - \xi_i^2) - \xi_i^2\left[\frac{1}{Q_e^2} - \frac{2}{\Lambda_f(\gamma_f + 1)}\right] S_A - \frac{2}{\Lambda_f(\gamma_f + 1)} S_B\right\} \quad (13)$$

$$C_{nf} = \{\tfrac{1}{2}(\gamma_f + 1)\Lambda_f\}^{1/(\gamma_f - 1)} \left\{\frac{(1 - \xi_i^2)(1 + Q_e^2)}{2} + \xi_i^2\left[\frac{1 + Q_e^2}{\Lambda_f(\gamma_f + 1)} - 1\right] S_A - \left[\frac{1 + Q_e^2}{\Lambda_f(\gamma_f + 1)} + \frac{\gamma_f - 1}{\gamma_f + 1}\right] S_B\right\} \quad (14)$$

where

$$\Lambda_f = 1 - Q_e^2(\gamma_f - 1)/(\gamma_f + 1)$$

$$S_A = \int_{\xi_i}^{1} \left(\frac{V_1^2}{\xi'}\right) d\xi'; \qquad S_B = \int_{\xi_i}^{1} V_1^2\, \xi'\, d\xi'$$

It can be seen that both C_{mf} and C_{nf} depend on S_A and S_B so that a universal swirl parameter cannot be defined, in contrast to the circular nozzle case, where only the second of these two integrals was present.[2]

For a nonswirling core flow, the mass flux and impulse function coefficients only depend on γ_c and W_c, but the latter depends on the level of swirl in the fan stream in the plane of the core nozzle exit. Considering the mass flux coefficient, this can be written as

$$C_{mc} = \{\tfrac{1}{2}[(\gamma_c + 1) - (\gamma_c - 1)\, W_c^2]\}^{1/(\gamma_c - 1)} W_c \quad (15)$$

where W_c is obtained from Eq. (3). To do this, however, we need to know the back-pressure ratio, which is determined by the static pressure in the fan stream at the core nozzle lip. This in turn depends on W_2^2 and V_2^2, which are given by Eqs. (4) and (5). In the small perturbation approximation, these are only required to $O(V_1^2)$, so that r_2 is needed only to $O(1)$; i.e., nonswirling values can be taken. This leads to the expression for core nozzle back-pressure ratio:

$$\left(\frac{p_{ex}}{p_0}\right)_c = \left(\frac{p_a}{p_0}\right)_c \left\{1 - \frac{\gamma_f}{\Lambda_f(\gamma_f + 1)}(2I_2 + V_{i2}^2 - V_{e2}^2)\right\} \quad (16)$$

where

$$I_2 = \int_{\xi_i}^{1} \frac{V_1 \xi'}{\xi'^2 - \xi_i^2 + \xi_{ex}^2} \frac{d(V_1 \xi')}{d\xi'} d\xi'$$

and $V_{e2}^2 = V_e^2/(1 - \xi_i^2 + \xi_{ex}^2)$ in the small perturbation approximation.

Thus, the core nozzle back-pressure ratio can be evaluated. If it is less than the critical value $(p_*/p_0)_c$, then $W_c = 1$ in Eq. (15); otherwise, Eq. (3) is used to find W_c. A similar procedure can be adopted to find C_{nc}, and then the four parameters can be substituted into Eq. (11) to find the thrust coefficient.

Nonuniform Stagnation Conditions

For the general case of nonuniform inlet conditions, the right-hand side of Eq. (1) becomes $dh_0/dr - T ds/dr$. Upon integrating across the nozzle exit, this gives Eq. (2), but with $S = S_1 - S_2 + S_3$, where S_1 was the original integral, and

$$S_2 = 2(h_{0e} - h_0)/a_{*e}^2$$

$$S_3 = \frac{2}{a_{*e}^2} \int_{r_1}^{R_e} T \frac{ds}{dr_1'} dr_1' \quad (17)$$

The variations of the thermodynamic properties across the nozzle exit can be expressed in terms of stagnation pressure variation. Thus,

$$\left(\frac{a_0}{a_{0e}}\right)^2 = \left(\frac{a_*}{a_{*e}}\right)^2 = \frac{T_0}{T_{0e}} = \frac{h_0}{h_{0e}} = \left(\frac{\rho_0}{\rho_{0e}}\right)^{\gamma - 1} = \left(\frac{p_0}{p_{0e}}\right)^{(\gamma - 1)/\gamma} \quad (18)$$

Furthermore, if the local departure of p_0 from p_{0e} is δp_0 (say), then

$$p_0/p_{0e} = 1 + \delta p_0/p_{0e} \quad (19)$$

Since a_* varies across the section in general, we write

$$q^2/a_*^2 = (W^2 + V^2)(a_{*e}/a_*)^2 \quad (20)$$

(as velocities are now nondimensionalized by a_{*e}) and

$$Q_e = \frac{\gamma + 1}{\gamma - 1}\left[1 - \left(\frac{p_a}{p_{0e}}\right)^{(\gamma - 1)/\gamma}\right]^{1/2} \quad (21)$$

We also require the isentropic flow relations

$$\left(\frac{a}{a_0}\right)^2 = \left(\frac{T}{T_0}\right) = \left(\frac{\rho}{\rho_0}\right)^{\gamma - 1} = \left(\frac{p}{p_0}\right)^{(\gamma - 1)/\gamma} = 1 - \frac{\gamma - 1}{\gamma + 1}(W^2 + V^2) - \frac{\gamma - 1}{\gamma + 1}(W^2 + V^2)\left\{\left(\frac{a_{*e}}{a_*}\right)^2 - 1\right\} \quad (22)$$

For simplicity, the entropy term is now dropped in what follows, but it could be handled in a similar fashion. At station 2 (Fig. 1), using conservation of vr and h_0 along streamlines, the velocity profiles are given by Eq. (6) (modified by the addition of $-S_2$ inside the square root sign) and Eq. (4). Equation (5) gives r_2, and, as before, this is solved iteratively using Eqs. (6) (modified), (4), and (18). The presence of the total enthalpy term on the right-hand side of Eq. (6) creates no special difficulty.

Small Perturbation Theory

Small perturbation expressions can be obtained, as before, by expanding and neglecting terms of $O(V_e^4)$. Thus, Eq. (2) becomes

$$W_1 = Q_e(1 - V_e^2/2Q_e^2 + S/2Q_e^2) + O(V_e^4) \quad (23)$$

where S is as given by Eqs. (17) and above. Equations (22) and (23) can now be combined to give an expression for ρ/ρ_0 in terms of S, swirl velocity, and $\{(a_{*e}/a_*)^2 - 1\}$, which is assumed to be $O(V_e^2)$.

The performance coefficients will involve terms such as $(\rho/\rho_{*e})_f$ as they are now nondimensionalized by critical conditions at the nozzle lip. This can be written

$$\frac{\rho}{\rho_{*e}} = \frac{\rho_{0e}}{\rho_{*e}} \frac{\rho_0}{\rho_{0e}} \frac{\rho}{\rho_0} \simeq \left(\frac{\gamma + 1}{2}\right)^{1/(\gamma - 1)} \left(1 + \frac{1}{\gamma}\frac{\delta p_0}{p_{0e}}\right) \frac{\rho}{\rho_0} \quad (24)$$

where subscripts f have been omitted for clarity.

Substituting Eqs. (23) and (24) into Eqs. (7) and (8) gives, upon integrating, expressions similar to Eqs. (13) and (14) but with the addition, inside the brackets on the right-hand side (with the S_A and S_B terms), of

$$[2 + (\gamma - 1)Q_e^2]/[\gamma(\gamma + 1)\Lambda] S_D$$

and

$$\frac{Q_e^2[3\Lambda\gamma - \Lambda + Q_e^2(\gamma + 1)] + [2\Lambda\gamma^2 + 3\Lambda\gamma + \Lambda - (\gamma + 1)]}{\gamma(\gamma + 1)\Lambda S_D}$$

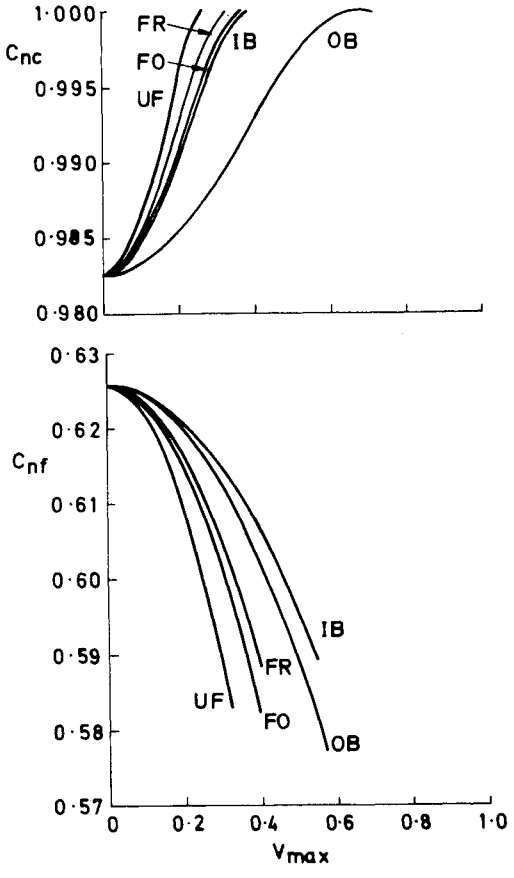

Fig. 4 Variation of nozzle impulse functions with swirl velocity for $V_F = 0.4847$, $(p_a/p_0)_{f,c} = 1/1.5$ (key as Fig. 2). Results of small perturbation theory.

(subscripts f have again been omitted for clarity) for C_{mf} and C_{nf}, respectively, where

$$S_D = \int_{\xi_i}^{1} \left(\frac{\delta p_0}{p_{0e}}\right) \xi d\xi \tag{25}$$

Equation (25) can easily be evaluated if we let

$$\delta p_0/p_{0e} = \pm(\Delta p_0/p_{0e})(1 - \xi_1)/(1 - \xi_i) \tag{26}$$

in which case

$$S_D = \pm(\Delta p_0/p_{0e})[(1 + \xi_i)/6 - \xi_i^2/3] \tag{27}$$

There is no need to assume such a linear profile; any specified profile of stagnation pressure can be accommodated and Eq. (25) integrated numerically. For the present purposes, however, we shall use Eq. (26) to illustrate the effects of p_0 gradients and swirl.

Results and Discussion

To assess the impact of swirl on nozzle performance using the present theory, swirl velocity profiles need to be specified at nozzle exit. Three families having linear variations with radius have been considered here; thus,

$$V_1 = V_i + (V_e - V_i)(\xi - \xi_i)/(1 - \xi_i) \tag{28}$$

The three families are referred to as inner-biased, uniform, or outer-biased swirl, depending on whether $(V_e - V_i)$ is negative, zero, or positive, respectively. These definitions differ from those used previously.[2]

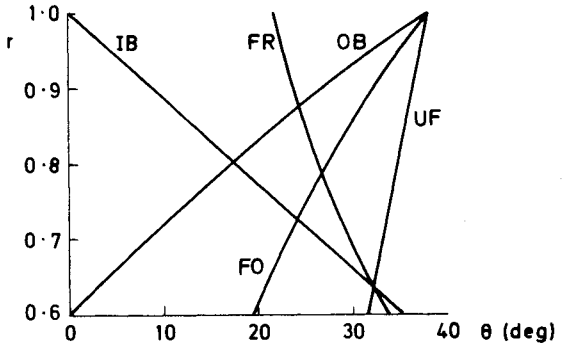

Fig. 5 Swirl angle profiles for $V_{max} = 0.5$, $p_a/p_{0f} = 1/1.5$ (key as Fig. 2).

Table 1 Engine parameters

R_e	R_i	R_{ex}	γ_f	γ_c	a_{*c}/a_{*f}	V_F
1.0	0.6	0.35	1.4	1.3	1.549	0.4847

Such linear profiles have been chosen to simplify the analysis while covering the likely range of swirl effects. To this end, a minimum swirl velocity of zero was used. Two other profiles have also been calculated, however. These are the forced vortex, a special case of the outer-biased family with $V_1 = V_e\xi$, and the free vortex, where $V_1 = V_i\xi_i/\xi$. (These swirl velocity profiles are shown in Fig. 2, together with the resulting axial velocity profiles.) The free vortex is of special interest, since in practice other swirl profiles tend to migrate toward this type for sufficiently long duct lengths. Analytically, however, it is a special case [as can be seen from Fig. 2 and Eq. (2)] and as such is not a good test of our theory.

The engine parameters that were used as the basis for the present calculations are given in Table 1. The value of V_F corresponds to a flight Mach number of 0.72. The present study was limited to swirl in the fan nozzle with nonswirling core nozzle flow, although swirl in either or both nozzles can be handled.[8] Both nozzles were taken to be operating at the same back-pressure ratio, with two values being used: $(p_a/p_0)_{f,c} = 1/1.89$ and $1/1.5$.

The effect of swirl on specific thrust is indicated in Fig. 3 for uniform stagnation pressure and two different back-pressure ratios. It can be seen that specific thrust decreases with increasing swirl and that the rate of decay depends on the swirl velocity profile. (Surprisingly, the free vortex and forced vortex produce almost identical thrust performances.)

The origins of the thrust loss can be found by examining Eq. (11) and Fig. 4. Although the core impulse function increases (until the core nozzle chokes), the fan impulse function falls faster. At the same time, the mass flux coefficients show similar trends to the respective impulse functions. Thus, fan mass flow decreases, but core mass flow increases until the nozzle chokes.

The other term in the thrust equation which is affected by swirl is the cowl pressure. This decreases with swirl. The present calculations have all assumed the cowl pressure to be the average of the pressures at the inner radii at planes 1 and 2. In practice the cowl pressure will vary with distance along the cowl in a fashion depending on cowl shape and swirl type. The other aspect of cowl flow which cannot be assessed here is afterbody friction drag. It is not clear how swirl will affect the cowl boundary layer.

From Fig. 3, it might at first sight appear that uniform swirl produces the greatest impact on thrust, with outer-biased swirl having the least effect. This comparison, however, has been made on the basis of maximum swirl velocity (V_{max}). A more common measure of swirl is the swirl angle, radial variations of which are shown in Fig. 5 for five different swirl velocity

profiles at a common V_{max}. When thrust coefficient is plotted against maximum swirl angle (θ_{max}) free and forced vortices are no longer indistinguishable, but uniform swirl continues to have the greatest impact and outer-biased swirl the least (Fig. 6).

In Fig. 7, thrust coefficient is plotted against a swirl parameter S'. This is the nondimensional angular momentum used by Kornblum et al.[13] and other workers. On this basis, the inner-biased profile is the worst and the forced vortex is the best, with uniform swirl producing a much better relative performance than before.

Which is the "right" swirl parameter? The answer depends on the context in which the question is posed. If one were interested in using swirl to reduce noise,[7] then a measure of noise attenuation would be the most appropriate swirl parameter. If the interest is in mass flow control,[8] then thrust should be plotted against mass flow change. The small perturbation analysis has shown [Eqs. (13) and (14)] that there is no compact "universal" swirl parameter, by contrast with the circular nozzle case,[2,5] and that the swirl parameter S' used by previous workers[13] is an entirely arbitrary choice.

We turn now to the effects of nonuniform stagnation conditions. Values for ΔP in the range ± 0.15 have been used to cover likely practical total pressure gradients. Baker[16] shows a realistic fan nozzle stagnation pressure profile close to $\Delta P = -0.14$ (but with the peak p_0 just inboard of the fan nozzle outer wall). Figure 8 illustrates the effect of stagnation pressure gradient on specific thrust coefficient for swirling and nonswirling flows at two different nozzle pressure ratios. From this it can be seen that the effects of swirl and stagnation pressure gradient are effectively additive. Thus, any thrust vs swirl curve will be displaced by the introduction of nonuniform p_0.

For these calculations, the average stagnation pressure ($\bar{p}_0$) was kept constant, where $\bar{p}_0$ was defined such that $\int p_0\, dr$ across the nozzle exit was the same for all profiles. Some additional calculations were also performed in which $\bar{p}_0$ was defined such that $\int p_0 r\, dr$ was constant, but these results differed little from the originals. In either case, the fan nozzle pressure ratio was $(p_a/\bar{p}_0)_f = (p_a/p_0)_c = 1/1.5$.

On this basis, the effect of a linear stagnation pressure gradient is to "rotate" the axial velocity profile in the same sense as p_0 (i.e., $\Delta P < 0$ increases W_1 at the outer radii), which agrees with Baker.[16] This has the effect of decreasing fan nozzle impulse function for $\Delta P < 0$ and decreasing mass flux, but by a lesser amount. The reverse applies for $\Delta P > 0$.

The effect of fan nozzle stagnation pressure gradients on the core nozzle performance is less straightforward. Increasing the *magnitude* of ΔP causes an increase in C_{mc} and C_{nc} at low swirls. At zero swirl, this increase depends only on $|\Delta P|$; this is because $p_{ex}/p_{0c} = (p_a/p_{0c})(1 - \Delta P^2)$ for zero swirl. As swirl velocity is increased, however, positive values of ΔP cause larger C_{mc} and C_{nc} increases than negative values. Thus, for outer-biased swirl at $V_{max} > 0.4$, there are larger C_{mc} and C_{nc} produced by $\Delta P = 0.1$ than by $\Delta P = -0.15$, with choking occurring at a slightly lower swirl level. As can be seen from Table 2, however, the overall fractional changes in core nozzle parameters decrease with increasing swirl (until they are zero at choking) and are, in any case, small by comparison with the changes in other parameters.

It should be pointed out that the analysis used here does not link any particular swirl profile with a stagnation pressure profile. This, it is felt, corresponds to a stagnation pressure gradient introduced by the fan with the swirl profile being produced (or, rather, modified from that at fan exit) by exit guide vanes.

In all the results discussed so far, it has been assumed that the total velocity remains constant along the fan jet outer boundary at a value determined by p_a/p_{0f}. In forward flight conditions, however, the external pressure at the fan nozzle lip may differ from ambient,[17] taking a value p_b, say. The thrust component that results from this is post-exit thrust[14] and has

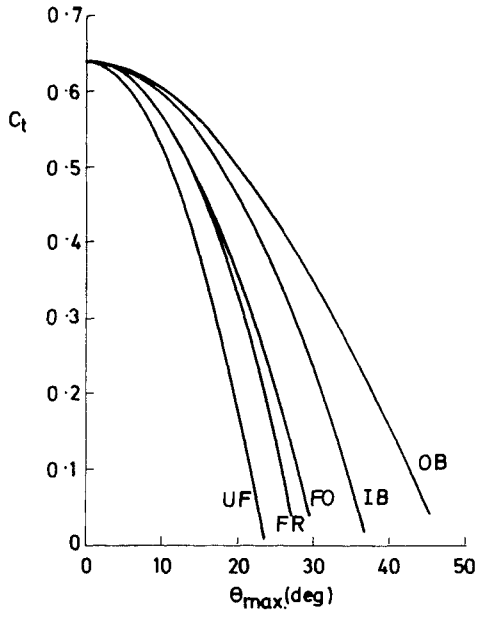

Fig. 6 Variation of thrust with swirl angle for $V_F = 0.4847$, $(p_a/p_0)_{f,c} = 1/1.5$ (key as Fig. 2). Results of small perturbation theory.

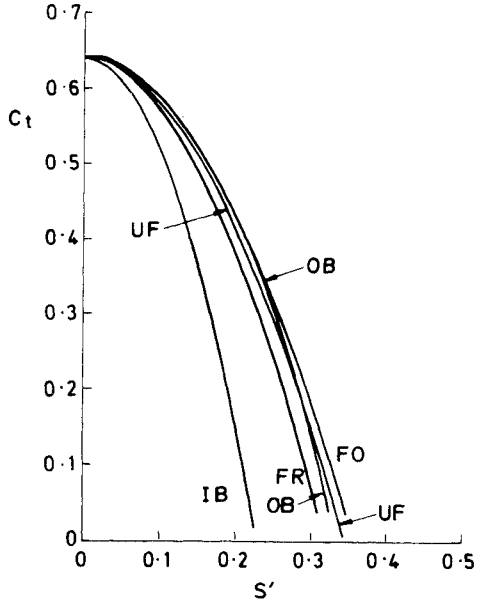

Fig. 7 Variation of thrust with swirl parameter S' for $V_F = 0.4847$, $(p_a/p_0)_{f,c} = 1/1.5$ (key as Fig. 2). Results of small perturbation theory.

Table 2 Effects of stagnation pressure gradients on engine performance parameters

Quantity	Value at $\Delta P = 0$	% change with: $\Delta P = 0.15$	% change with: $\Delta P = -0.15$
Nonswirling flow:			
C_{mf}	0.6122	+ 15	− 11.5
C_{nf}	0.6259	+ 19.5	− 21
C_{mc}	0.9653	+ 0.8	+ 0.8
C_{nc}	0.9826	+ 0.4	+ 0.4
p_{cowl}	0.6667	+ 23.6	− 21.4
Swirling flow ($V_{max} = 0.5$, outer-biased):			
C_{mf}	0.5778	+ 15	− 12
C_{nf}	0.5889	+ 20.6	− 22.2
C_{mc}	0.9940	+ 0.4	+ 0.1
C_{nc}	0.9968	+ 0.2	+ 0.1
p_{cowl}	0.6154	+ 23.8	− 21.5

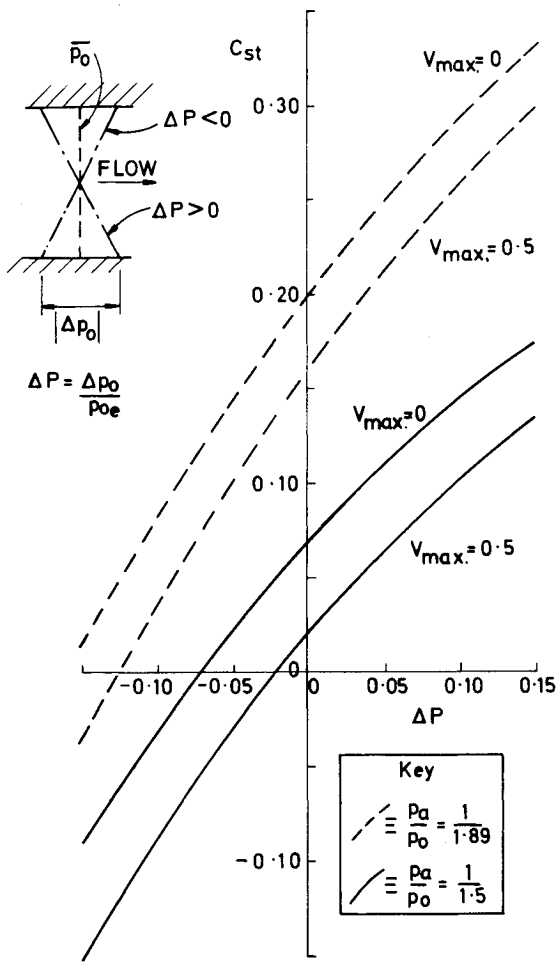

Fig. 8 Variation of specific thrust with total pressure gradient for outer-biased swirl with $V_F = 0.4847$. Results of small perturbation theory.

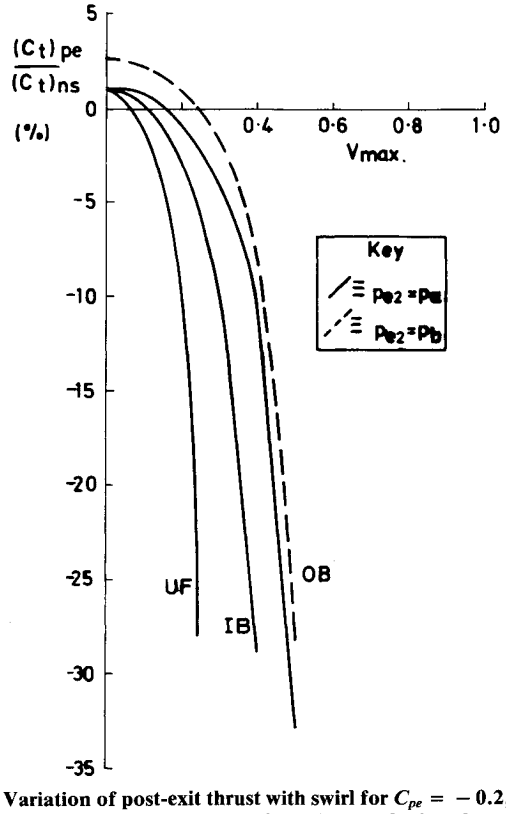

Fig. 9 Variation of post-exit thrust with swirl for $C_{pe} = -0.2$, $V_F = 0.4847$, $(p_a/p_0)_{f,c} = 1/1.5$. Results of small perturbation theory.

previously been shown to be small for supercritical jets.[3] For the present case, post-exit thrust can be estimated for any given p_b, provided that the pressure acting on the outside of the fan stream at plane 2 (p_{e2}) can be specified. If it is then assumed that adjustment between plane 2 conditions and ambient conditions at downstream infinity takes place isentropically,[14,3] then post-exit thrust can be determined.

Calculations have been performed based on two different assumptions for p_{e2}. The first assumption was that ambient pressure was reached on the jet boundary by plane 2, and the second assumption was that $p_{e2} = p_b$. In both cases, $p_b/p_a = 0.929$, which corresponds to $C_{pe} = -0.2$. Post-exit thrust was calculated as the difference between total thrust and net standard thrust, where total thrust is determined by considering momentum balance for a control volume that extends to downstream infinity.

Results are presented in Fig. 9, from which it can be seen that there is little difference between the two assumptions for p_{e2} at high swirls, compared with the effects of swirl itself. Initially, post-exit thrust is small and positive, due to the increased fan stream impulse function in the presence of the lower fan nozzle back pressure. Mass flux also increases (compared with ambient back pressure), but this is a smaller (negative) component of thrust. Post-exit thrust decreases with swirl, in contrast with earlier findings for supercritical jets.[3] At high swirl levels it becomes fairly large and negative, contributing a drag component that cannot be neglected. This is primarily due to the increase in fan nozzle mass flow (intake momentum drag) in the presence of the reduced back pressure. Thus, when considering total thrust variation with swirl, the falloff will be even more dramatic than that shown in Figs. 3, 6, and 7 (for a cowl shape giving $C_{pe} \simeq -0.2$). The relative performance of the various swirl profiles, however, does not seem to change when post-exit thrust is taken into account.

It should be pointed out that most of the results presented here are of calculations at the high back-pressure ratio (1/1.5). As can be seen from Fig. 3, this exaggerates the *percentage* change in thrust. Furthermore, the small perturbation theory has been used for most cases presented here, and, as also shown in Fig. 3, this slightly overestimates the thrust loss at high swirl levels but by an amount that depends on nozzle pressure ratio and is thus smaller at the higher back-pressure ratio used here. Also, streamline curvature is neglected, and this tends to oppose swirl in its effects.

Conclusion

A quasicylindrical theory has been developed for subcritical, swirling flows in annular nozzles. A small perturbation theory, which involves even less computational time, has also been developed. This has been shown to give good agreement with the more accurate approach, even for quite high swirl levels, particularly for higher back-pressure ratios.

Using these theories, it has been shown that thrust decays with swirl at a rate that depends on the swirl profile (radial variation of swirl velocity). The swirl profile giving the lowest thrust loss depends on the basis of comparison, which in turn depends on the context in which the question is posed. No compact "universal" swirl parameter exists for this case.

The loss of thrust is primarily due to the reduction in fan nozzle impulse function and lowered pressure on the afterbody cowl. The increase in core nozzle impulse function due to the lower back pressure caused by swirl is insufficient to compensate for this loss for the type of engine studied here.

Both the quasicylindrical and small perturbation theories have been extended to allow for radially nonuniform stagnation pressure. Calculations for linear p_0 profiles have shown that thrust decreases as the profile becomes more outer-biased (higher p_0 at higher r) but increases for inner-biased p_0 profiles. Outer-biased profiles are more likely to occur in practice, since these correspond to high-work fan tip sections.

As with swirl, the major impact of stagnation pressure gradients is on fan nozzle impulse function and afterbody

cowl pressure. Swirl has an approximately additive effect on thrust in the presence of nonuniform stagnation conditions.

Finally, the impact of post-exit thrust has been estimated for a typical pressure coefficient at the trailing edge of the fan cowl. Although this thrust component amounts to less than 3% of net-standard thrust in the absence of swirl, increasing swirl causes decreasing post-exit thrust until it becomes a substantial drag component.

It is felt that the methods presented here could be of particular benefit to the propulsion community. They provide a quick, cheap means of determining the effect on thrust of swirl and stagnation pressure gradients. The absence of viscous effects in the present calculations could be a useful feature, since comparisons of these calculations with those obtained from a viscous code could distinguish viscous effects from essentially inviscid ones. Streamline curvature tends to ameliorate the effects shown here, and so the present results are pessimistic.

References

[1]Carpenter, P. W. and Johannesen, N. H., "An Extension of 1-D Theory to Inviscid Swirling Flow through Choked Nozzles," *Aeronautical Quarterly,* Vol. 26, May 1975, pp. 71–87.

[2]Carpenter, P. W., "A General One-Dimensional Theory of Compressible Inviscid Swirling Flows in Nozzles," *Aeronautical Quarterly,* Vol. 27, Aug. 1976, pp. 201–216.

[3]Carpenter, P. W., "The Effects of Swirl on the Performance of Supercritical Convergent-Divergent Nozzles," *Aeronautical Quarterly,* Vol. 32, May 1981, pp. 126–152.

[4]Carpenter, P. W., "Supercritical Swirling Flows in Convergent Nozzles," *AIAA Journal,* Vol. 19, May 1981, pp. 657–660.

[5]Carpenter, P. W., "Effects of Swirl on the Subcritical Performance of Convergent Nozzles," *AIAA Journal,* Vol. 18, May 1980, pp. 600–602.

[6]Carpenter, P. W., "A Linearised Theory for Swirling Supersonic Jets and its Application to Shock-Cell Noise," *AIAA Journal,* Vol. 23, Dec. 1985, pp. 1902–1909.

[7]Schwartz, I. R., "Minimization of Jet and Core Noise of a Turbojet Engine by Swirling the Exhaust Flow," AIAA Paper 75-503, March 1975.

[8]Knowles, K. and Carpenter, P. W., "The Use of Swirl to Control the Flow Rate through the Propulsion Nozzles of Turbofan Aero-Engines—A Feasibility Study," Univ. of Exeter, School of Engineering, Exeter, UK, TN 82/3, 1982.

[9]Lewellen, W. S., Burns, W. J., and Strickland, H. J., "Transonic Swirling Flow," *AIAA Journal,* Vol. 7, July 1969, pp. 1290–1297.

[10]Gostintsev, Y. A., Zaitsev, V. M., and Novikov, S. S., "The Thrust of a Nozzle with a Swirling Gas Flow," *Izvestiya Akademii Nauk SSSR, Mekhanischeskaya Zhidk. i Gaza,* No. 5, 1975, p. 145 (in Russian).

[11]Pandolfi, M., "Transonic Swirling Flow in Axisymmetric Nozzles," *Meccanica,* Vol. 11, No. 3, 1976, pp. 157–161.

[12]Smith, R, "An Investigation of the Effects of Swirl on Some Flows at Transonic, Supersonic and Hypersonic Speeds," Ph.D. Thesis, Univ. of Manchester, Manchester, UK, 1971.

[13]Kornblum, B. T., Thompson, H. D., and Hoffmann, J. D., "An Analytical Investigation of Swirl in Annular Propulsive Nozzles," *Journal of Propulsion and Power,* Vol. 2, March–April 1986, pp. 155–160.

[14]Mair, W. A., et al., "Definitions of the Thrust of a Jet Engine and of the Internal Drag of a Ducted Body," *Journal of the Royal Aeronautical Society,* Vol. 59, No. 536, 1955, pp. 517–526.

[15]Knowles, K. and Carpenter, P. W., "A Quasi-Cylindrical Theory for Swirling Flow in Annular Nozzles," Univ. of Exeter, School of Engineering, Exeter, UK, TN 81/13, 1981.

[16]Baker, T. J., "The Computation of Transonic Potential Flow," *Computational Methods for Turbulent Transsonic and Viscous Flows,* edited by J. A. Essers, Hemisphere, Washington, DC, 1983, pp. 213–289.

[17]Bowers, D. L. and Tamplin, G., "Throttle-Dependent Forces," *Thrust and Drag: Its Prediction and Verification,* edited by E. E. Covert, AIAA, New York, 1985, pp. 207–280.